ARTICLE

Recent progress on the development of porous carbon-based electrodes for sensing applications

Received 00th January 20xx,
Accepted 00th January 20xx

DOI: 10.1039/x0xx00000x

Ana Casanova, [a] Jesus Iniesta [b,c] and Alicia Gomis-Berenguer *[c]

Electrochemical (bio)sensors are considered a clean and powerful analytical tool capable to convert an electrochemical reaction between analyte and electrode into a quantitative signal. They are an important part of our daily lives integrated in several fields such as healthcare, food and environmental monitoring. Several strategies to improve its sensitivity and selectivity have been applied in the last decades, including the incorporation of porous carbon materials in its configuration. Porosity, surface area, the graphitic structure as well as the chemical compositon of the materials greatly influence the electrochemical performance of the sensors. In this review, activated carbons, ordered mesoporous carbons, graphene-based materials, and MOF-derived carbons, which are used to date as crucial element of electrochemical device, are described from its textural and chemical composition to its role in the outcome of electrochemical sensors. Several relevant and meaningful examples about materials synthesis, sensors fabrication and applications are illustrated and described. The closer perspectives on these fascinating materials forecast a promising future for the electrochemical sensing field.

1 Introduction

Carbon materials have been devoted a wide range of electroanalytical applications due to their unique properties. They exhibit chemical stability, relatively wide potential window in aqueous solutions, low background signal and fast electron transfer rates.[1,2] Graphite, carbon nanotubes, graphene, carbon black or carbon nanofibers correspond to several examples of carbon materials used for the design of electrochemical sensors and biosensors.[3-6]

According to the IUPAC definition, an electrochemical sensor is classified as sub-group of chemical sensor, where the function of the transducer is the transformation of the electrochemical interaction between analyte-electrode into a useful electrical signal.[7] In recent years, electrochemical sensors have played a key role in the achievement of more robust and successful analytical tools. This fact is closely related to the complementarity of the physico-chemical properties of the materials used for their manufacture, with their interaction with the analyte and/or biological species, conferring these analytical platforms suitable qualities for the improvement of technology in fields of food industry, environmental and healthcare, essential in the everyday life.[8]

Figure 1 collects a timeline of the use of selected carbon materials as a component of electrochemical sensor, indicating the first paper reported on the application of each carbon material as a core element of an efficient sensor towards different analytes.[9-18] As can be seen in Figure 1, in the last 20 years, an increasing trend of the use of carbon materials as a crucial component of electrochemical (bio)sensor has emerged due to the fast evolution of the synthesis methods and the deeper knowledge and control of carbon structures in terms of synthesis and characterization.

Beyond the high electronic conductivity and good chemical stability, the porous structure of some carbon-based materials allows the development of enhanced electrochemical response.[19] A porous material is defined as a solid composed of an interconnected network of pores filled with a liquid or gas, and gas adsorption is the well-established tool for its textural characterization. According to the pore size, the structure may consist of micro- (diameter < 2 nm), meso- (2-50 nm) and/or macropores (> 50 nm).[20] Generally, while micro- and mesoporosity provide a high surface area, the meso- and macropores facilitate the molecules access to the inner surface. Indeed, not only carbon materials have been employed for successfully fabrication of sensors, a plethora of porous materials has been used for this purpose including conductive polymers, hydrogels or porous silica.[21-23]

[a] Department of Chemistry, School of Engineering Science in Chemistry, Biochemistry and Health, Royal Institute of Technology, KTH, SE-100 44 Stockholm, Sweden.
[b] Department of Physical Chemistry, University of Alicante, 03080 Alicante, Spain.
[c] Institute of Electrochemistry, University of Alicante, 03080 Alicante, Spain.

The accessible porous network and large surface areas of porous carbon structures confer to the carbon-based modified electrode an important electroactive area (much higher than the underlying electrode) originating generally, a greater capacitive current intensity.[24,25] By considering irreversible redox reactions, the electrochemical response of analytes onto porous carbon-based modified electrodes will be dominated by the rate of electron transfer between the electrode and analyte. The enhanced interaction and the attractive electronic properties of the carbonaceous material may provoke an improvement of charge transfer kinetics leading to higher peak currents (also associated to the preconcentration effect) and lowering overpotentials. The electrochemical properties displayed by porous carbon materials are ensuring the fast charge transfer processes, and they are strongly dependent on the carbon network, pore characteristics (*e.g.*, more or less connected structures, pore sizes, etc.), or their surface chemistry.

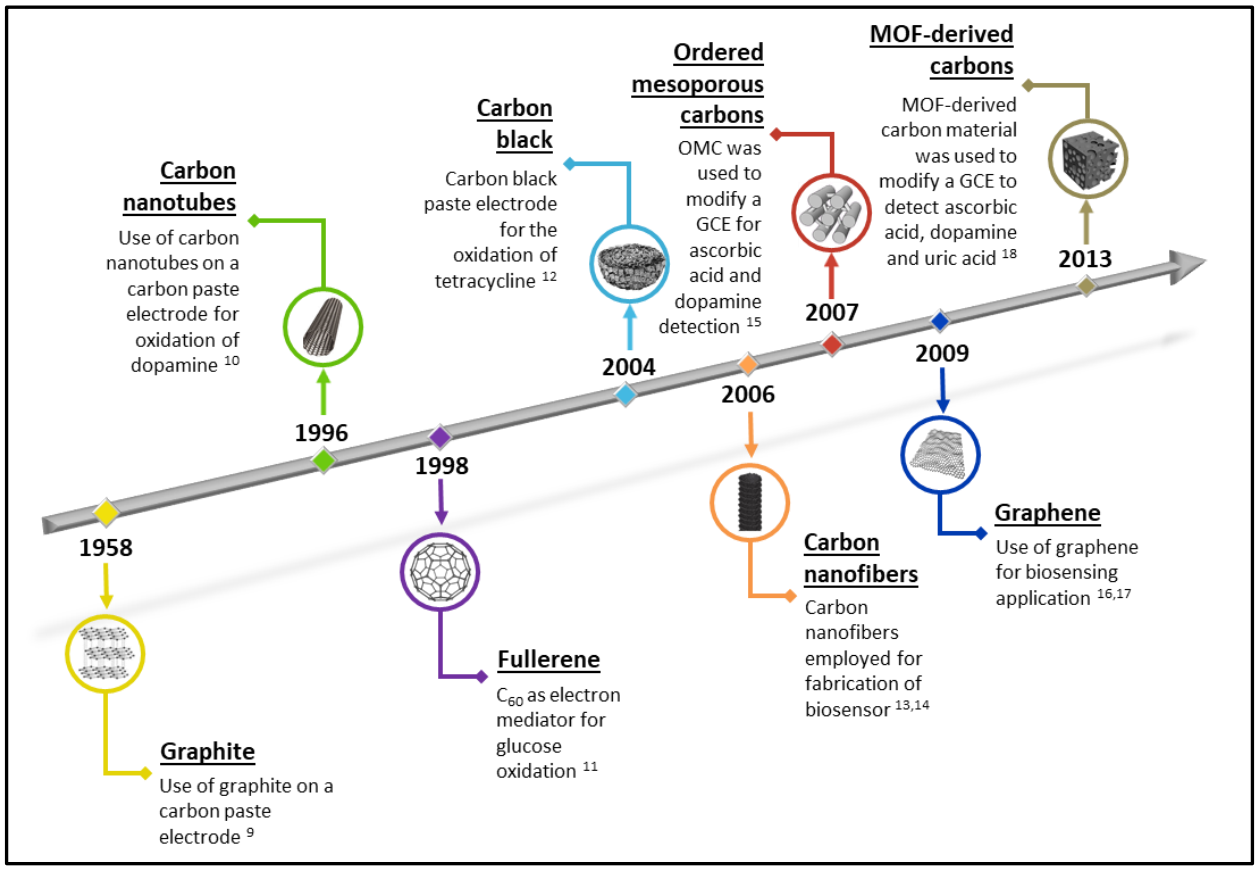

Fig. 1. Timeline reflecting the first work reporting the employ of selected carbon materials to fabricate an electrochemical (bio)sensor.

Regarding the chemical composition, the heteroatom-doped carbon skeleton has led to significant improvements in the selectivity of the detection.[26,27] Porous carbon materials can be functionalized by well-established reactions[28-30] and the attached functional groups provide active sites for the immobilization of biomolecules (*e.g.*, enzymes, proteins, nucleic acid-based receptors) with greater stability, reproducibility and sensitivity, assuring the carbon-analyte interaction inside the pores.[31,32] Furthermore, the high biocompatibility of carbon materials ensures the stability and biochemical function of the retained bioreceptors.

Accordingly, in order to choose the most efficient carbon material to fabricate a competent porous carbon-based modified sensor, it is necessary to understand: (i) the material's porosity, (ii) the surface chemistry and defects on the carbon surface, (iii) the chemical nature of the bioreceptor or electroactive species and, (iv) the characteristics of the analyte to be detected. The synergy of all these parameters will contribute to high sensitivities, low detection limits and wide linear concentration ranges of electrochemical sensors.

Overall, this work is intended to critically feature the recent advances, published during the last 10 years, on the use of porous carbon materials for the fabrication of carbon-based modified sensing devices. The review will focus on the purely carbonaceous materials, not the composites (such as oxide/carbon material[33-36]) and not the metal/carbon materials (such as metal nanoparticles/carbon materials[37-40]). Accordingly, the review starts with some generalities on the use of carbon materials to fabricate modified electrodes, followed with a description of the most widely used electrode configurations and its preparation mode. Then, different sections are reported on the basis of selected porous carbon materials (*i.e.*, activated carbons, ordered mesoporous carbons, graphene-based materials, and metal organic framework (MOF)-derived carbon materials) applied in several

sensing devices for a wide variety of configurations and analytes.

The role of the porous carbon material as mediator, transducer or adsorbate will be described as a function of the carbon origin, with particular attention to their porous structure and chemical composition. Rather than citing an extensive number of works (Tables 1-4), only some selected and significant ones are described in this review.

Despite a high number of interesting reviews and books published in the last decades covering electrochemical sensors based on carbon materials,[1,3,4,6,19,41-44] the present one is the first comprehensive report collecting exclusively porous carbon materials (based on their origin) as a component of the electrochemical device to improve the sensors performance and outcome. Overall, this review supplies the reader with a general perspective of scientific community and significant insights into improving the analytical performance of (bio)sensors by its modification with a wide variety of porous carbon materials.

2 Carbon materials for sensing applications

Different electrode materials have been employed as transducer to fabricate an electrochemical sensor, being the most common the metal electrodes and carbon-based electrodes. The last ones have the advantage over the first that they exhibit significantly lower background currents. The use of carbon-based electrodes was reported for the first time by Adams in 1958[9] who published the employment of a carbonaceous paste (*i.e.*, a mixture of graphite powder and a binder) as electrode (carbon paste electrode, CPE) to detect the oxidation of iodide ion. Since this achievement, different carbon powders, including porous carbon materials, have been used for the fabrication of CPE.[44-47] The physico-chemical features of the carbonaceous materials have a strong influence on the properties of the obtained CPE and on its application. Beyond the carbon paste, other electrode configurations (considered as carbon ink-based electrodes) have emerged as attractive alternative to construct robust, reproducible and low-cost carbon-based sensors. They include the screen-printed electrodes (SPEs),[1,48,49] paper-based electrodes,[50,51] carbon thin films sensors,[52-54] and so on. Additionally, the glassy carbon electrode (GCE) is the most used carbon-based electrode to be modified for electrochemical sensing applications.

Most electrochemical (bio)sensors are based on chemically and/or biologically modified electrodes that are constructed with: (i) a conducting material (*e.g.*, carbon-based electrode or metal), which acts as transducer, and (ii) a modifier (*e.g.*, porous carbon-based material), which interacts with the bioreceptor (electrochemical biosensor) or directly with the target molecule (electrochemical sensor). A scheme of a (bio)sensor modified with carbon material and its transducing mechanism is showed in Figure 2.

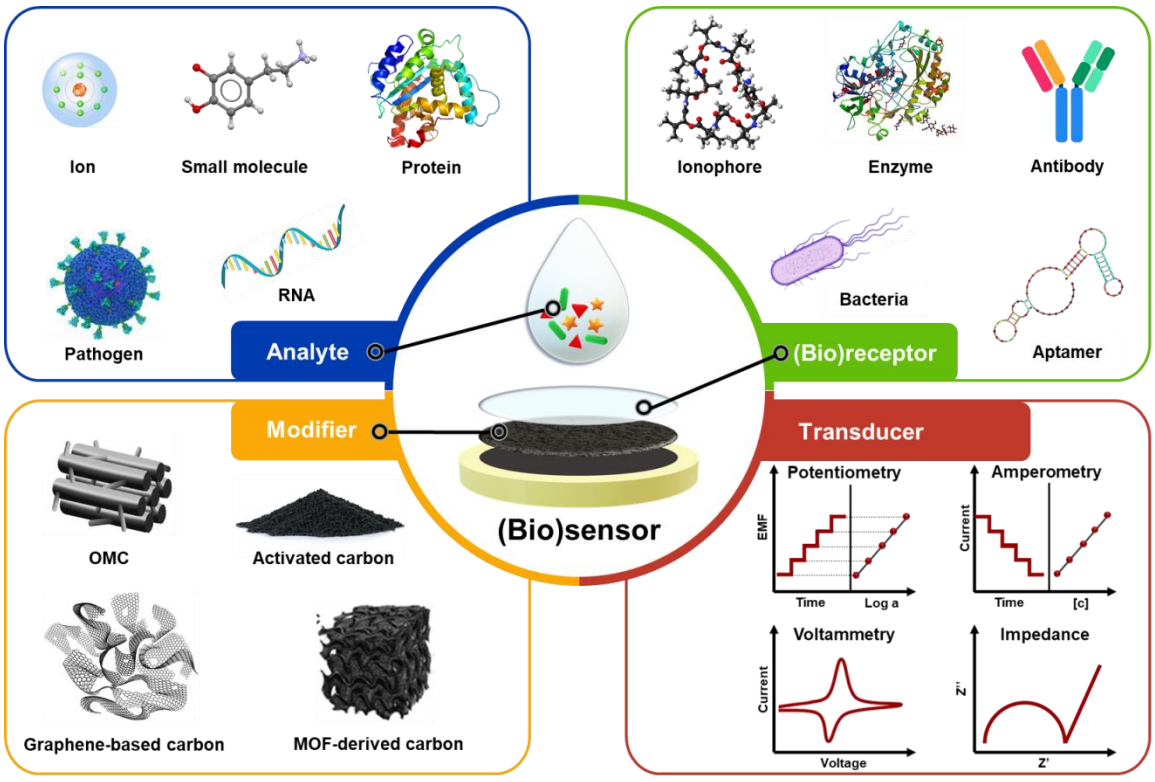

Fig. 2. Scheme of (bio)sensor indicating its different components with several examples.

Several ways for the fabrication of carbon-based modified electrodes have been reported during the last decades, pointing out the impact of the electrode type and its modification on the final device efficiency. In this sense, the above-described CPE was obtained by mechanical mixing of carbon material and/or graphite powder, and a mineral oil (usually in proportions as 10-20, 60-40 and 30-40 wt.%, respectively). The surface of the electrode can be renewed by mechanical polishing to remove the used surface.[44] The SPEs emerged as alternative to CPE, the former are electrochemical devices manufactured by printing an ink on a plastic or ceramic inert substrates. Its modification is possible either by casting onto the working electrode surface of a carbon dispersion solution (*e.g.*, in ethanol, isopropanol or dimethylformamide) or by the reformulation of the carbon slurry and, then manually or mechanically printed through the inert platform. Another strategy to get a carbonaceous modified electrode corresponds to the modification of a conductive substrate (generally a GCE or disc electrode), by drop-casting, with a carbon material dispersion.

Consequently, a wide variety of porous carbon-based materials has been used for electrochemical (bio)sensors fabrication. To this purpose, in this review some porous carbon materials have been selected, and a plethora of applications are described in detail, by making a journey from the conventional and well-known activated

carbons to the relatively new MOF-derived porous carbon materials.

2.1 Activated carbons and chars

Activated carbons (AC) derived from lignocellulosic biomass are widely used for a pool of applications in different fields ranging from energy storage,[25,55] and catalysis[56,57] to environmental remediation.[58] They are obtained by a so-called activation method (i.e., physical and chemical activation) that consists on a carbonization or oxidation step of the precursor, followed by the exposure of the carbonized material to a reactive atmosphere in the presence of activating agent that allows the development of a porous structure. The greatest advantage of activated carbons is that they can be generated from biomass waste (cost-effective precursor) and the obtained material will show a high porosity after appropriate activation process. The control of synthesis conditions, such as the biomass precursor, the carbonization process and the activation procedure (including the control of activating agent, precursor/activating agent ratio, temperature, dwelling time, etc.) will determine the final properties of such carbonaceous material.

More recently, activated carbons and biochars (carbon-rich product formed by thermal decomposition of biomass) have been employed for the modification of chemical sensors in view of their reduced environmental footprint, low-cost and the combination of different physico-chemical properties.[42,59] In this regard, it was reported several examples of electroanalytical devices constructed with activated carbons, from different carbon sources, showing good performances for the detection of biomolecules,[60-64] pharmaceuticals,[65,66] pesticides,[67,68] and metals[69-71] (Table 1). Some selected recent reports are briefly described hereafter.

Lu and co-workers investigated the use of amorphous carbon material obtained by carbonization of lotus steam to develop an electrochemical sensor for the simultaneous determination of hydroquinone, catechol and nitrite.[72] The porous structure with a pore size distribution centered at 3.0-4.5 nm enhanced the electron transfer rate on the modified electrode allowing such a meaningful simultaneous determination of the three compounds (Figure 3a).

Akshaya *et al.*[73] developed a non-enzymatic electrode modified with mesoporous carbon nanospheres obtained from onion peels. The obtained porous material was coated on a toray carbon fiber paper to reach a 1 cm^2 electrode. They reported the quantification of progesterone in human blood, serum and milk samples at picomolar level. The good sensitivity was ascribed to the porosity and open-pore network of the obtained nanospheres, which facilitate faster molecular diffusion and promote the electrooxidation of progesterone.

Veeramani and co-workers[74] studied the use of a biomass derived carbon material. The authors carried out the activation of *Bougainvillea spectabilis* flower with $ZnCl_2$ as activating agent and pyrolyzed at 800 °C. The obtained micro-mesoporous activated carbon with a specific surface area of 1197 m^2/g was coated on the GCE and employed as a sensor for the detection of catechin (antioxidant belonging to the flavonoids family) by applying differential pulse voltammetry (DPV). Results showed that the presence of the activated carbon improves the diffusion process, letting the formation of a well-resolved and sharp oxidation peak associated to the oxidation of catechin to quinone derivative. A similar strategy was followed by Kim *et al.* who developed a sensor for acetaminophen (paracetamol) determination by using DPV.[75] They fabricated a modified electrode casting an activated carbon slurry on the GCE. The carbonaceous material was obtained from seaweed by a two-step activation using $ZnCl_2$ and KOH, respectively. A satisfactory sensitivity and selectivity were obtained mainly associated to the high electrochemical surface area of the carbon-modified electrode (0.122 cm^2) caused by the activation protocol.

Several porous carbon materials have been employed to immobilize redox proteins and enzymes, where a paradigm of such as biospecies applies the use of glucose oxidase (GOD) immobilized on the porous carbon-based electrode surface towards glucose biosensing.[76-80] Recently, Shan and co-workers[81] reported an elegant biosensor based on a carbonaceous support for loading GOD enzyme. They prepared a carbonaceous material (named as 3D-CVS) by carbonization of dried cane vine stem from Wisteria plant, a cylindrical morphology of carbon material with a three-dimensional micro-, macroporous structure was obtained. The cylindrical shape was fitted into a pipette and carbonaceous ink was used to make electrical contact (Figure 3b). GOD was adsorbed on the 3D porous structure allowing the quantification of glucose

through the O_2 reduction reaction as written in the form: glucose + O_2 + GOD → gluconolactone + H_2O_2. An increase of glucose concentration provoked a decrease of cathodic peak current, obtained by DPV. The good response of the biosensor was associated to the well immobilization of GOD on the tip, due to the presence of some defects, pores, and nitrogen-containing groups on the material surface. The immobilization enhanced the mass diffusion and electron transfer facilitating the catalytic oxidation of glucose.

Table 1. Figures of merit of selected activated carbons and biochars employed for the fabrication of electrochemical (bio)sensors.

Material	Type of porosity	Analytes	Concentration range	LOD	Sample	Technique	Ref.
AC	Microporous	Caffeine	39.8-637 µM	16 µM	Commercial beverages	DPV	60
AC	Microporous	Tryptophan	1-103 µM	30 nM	Pharmaceutical	Amperometry	61
AC	Microporous	Ascorbic acid Dopamine Uric acid	0.05-200 µM 2-2000 µM 1-2500 µM	0.02 µM 0.16 µM 0.11 µM	Urine	DPV	62
AC	n.r.	Puerarin	0.24-15.4 µM	0.064 µM	Pharmaceutical	DPV	63
AC	Hierarchical (micro-, meso-, macroporous)	Ascorbic acid Dopamine Uric acid Nitrite	(33-166), (166-26.47) µM (1.6-72), (82-2630) µM 1.6-4134 µM 4.9-1184 µM	13.7 µM 3.3 µM 1.1 µM 2.7 µM	Urine	Amperometry	64
AC	n.r.	Acetaminophen	0.1-1000 µM	0.054 µM	Blood, pharmaceutical	DPV	65
AC	n.r.	Dopamine Acetaminophen Salicylic acid	0.1-1000 µM	0.0313 µM 0.0282 µM 0.0487 µM	Blood, pharmaceutical	DPV	66
AC	n.r.	Methyl parathion	0.1-70 µM	0.039 µM	Drinking water	DPAdSV	67
AC	n.r.	Paraquat	0.03-1 µM	0.0075 µM	Coconut water, natural water	DPAdSV	68
AC	Hierarchical (micro-, meso-, macroporous)	Cd^{2+} Pb^{2+} Cu^{2+} Hg^{2+}	0.39-6.1 µM 0.49-7.41 µM 0.99-12.3 µM 0.99-9.91 µM	0.0041 µM 0.0072 µM 0.0791 µM 0.0065 µM	Synthetic samples	DPV	69
AC	Micro-, mesoporous	Pb^{2+} Cd^{2+}	0.025-0.500 µM 0.025-0.500 µM	0.01012 µM 0.0267 µM	Synthetic samples	SWASV	70
AC	Microporous	Pb^{2+}	2-120 µM	0.7 µM	Tap water	DPASV	71
Biochar	Micro-, mesoporous	Hydroquinone Catechol Nitrite	1-700 µM 1-3000 µM 0.5-4000 µM	0.15 µM 0.11 µM 0.09 µM	Tap water	Amperometry	72
Biochar	Mesoporous	Progesterone	0.037-0.25 nM	0.012 nM	Human blood, serum, cow milk, injections	CV, DPV	73
AC	Micro-, mesoporous	Catechin	4-368 µM	0.67 µM	Green tea leaves	DPV	74
AC	Micro-, mesoporous	Acetaminophen	0.01-20 µM	0.004 µM	Urine	DPV	75
Biochar	Micro-, macroporous	Glucose	0.58 µM-16 mM	0.19 µM	Blood serum	DPV	81
AC	Hierarchical (micro-, meso-, macroporous)	Furazolidone	0.5-270 µM	0.5 nM	Urine	Amperometry	82
AC	Micro-, mesoporous	4-Chlorophenol	50-500 µM	2.38 µM	Synthetic samples	CV	83

n.r.: non-reported

With respect to the role of functional groups of carbonaceous modifier, Ramadhass and co-workers reported the use of 3D honey-comb like nitrogen self-doped activated carbon to modify a GCE.[82] They described the quantification of furazolidone (antibiotic drug) showing a cathodic peak current (obtained from cyclic voltammetry, CV) about 7 folds higher than the bare GCE. Their experiments revealed that at pH 5 the interaction between the protonated nitro group of the analyte and the -OH, -C=O and -NH functional groups of the activated carbon surface enhance the furazolidone adsorption reducing the diffusion path and improving the electrocatalytic activity of the sensor showing a limit of detection (LOD) of 0.5 nM.

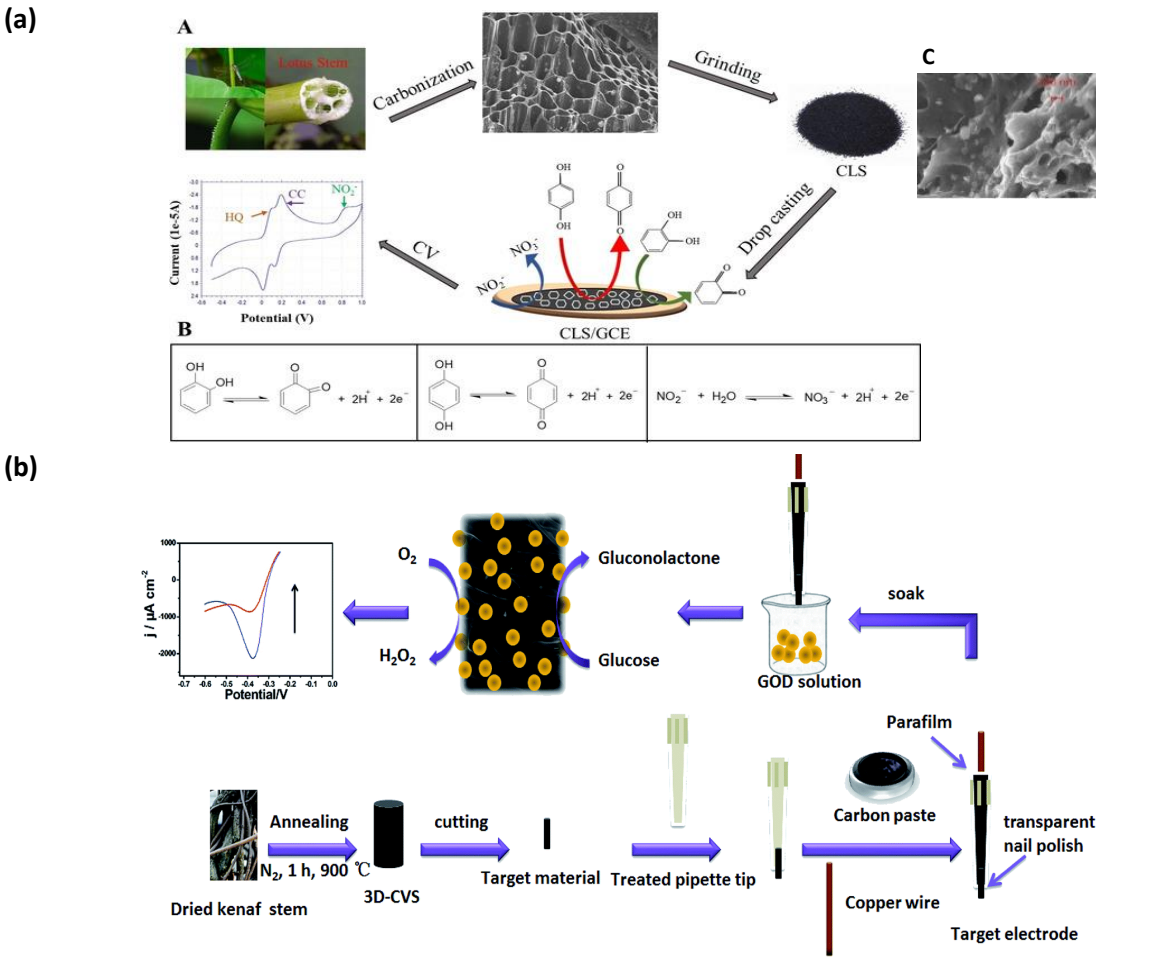

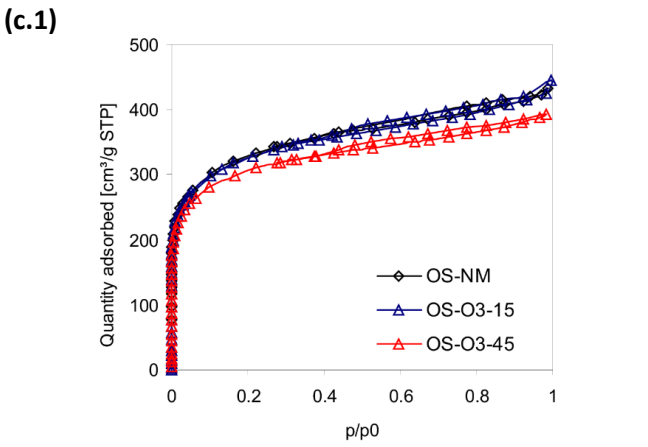

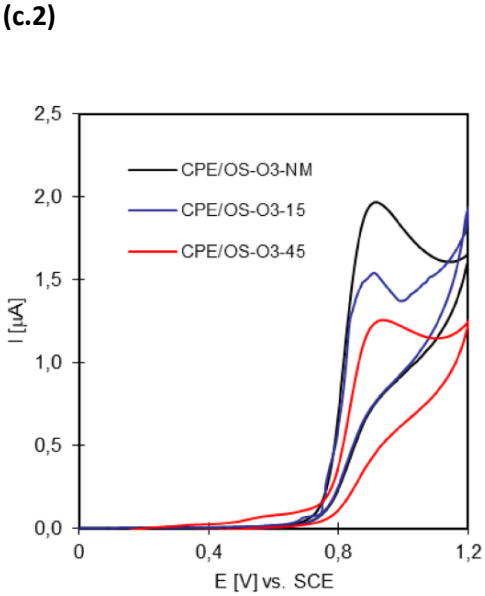

Activated carbon	S_{BET} (m^2/g)	V_t (cm^3/g)	Oxygen (EDS)	
			(% at.)	(% mass)
OS-NM	1138	0.549	2.88	3.74
OS-O3-15	1129	0.542	5.66	7.04
OS-O3-45	1055	0.491	6.22	8.42

Fig. 3 (a) A. Illustration of the fabrication and application of the carbonaceous sensor, B. sensing mechanism and C. SEM image of grinded porous material. (Reproduced from ref. 72). **(b)** Scheme of synthesis of 3D porous cane vine steam-derived carbon material (3D-CVS) and sensor preparation; reproduced from ref. 81. **(c.1)** N_2 adsorption/desorption isotherms at 77 K of OS-NM, OS-O3-15 and OS-O3-45. Table of textural parameters (S_{BET}-specific surface area and V_t-total pore volume) and oxygen content of the studied samples. **(c.2)** Cyclic voltammograms for CPEs modified in 0.5 mM of 4-chlorophenol. (Reproduced from ref. 83).

On other work, various oxidized activated carbons, obtained by ozone treatment during 15 and 45 min (samples named OS-O3-15 and OS-O3-45, respectively) of demineralized commercial carbon (sample OS-NM) were tested to modify a CPE.83 These materials presented quite similar textural properties, but with significant differences in their oxygen content following the trend OS-O3-45 > OS-O3-15 > OS-NM (Figure 3c.1). The authors reported the maximum sensitivity towards 4-chlorophenol electrochemical oxidation for the less oxidized activated carbon (OS-NM) (Figure 3c.2), showing a LOD 30 times lower than the bare CPE. This fact was directly correlated with the decrease of adsorption efficiency when the oxygen content was increased (decrease on the hydrophobicity character reducing the dispersive forces between graphene layers and analyte). Additionally, the electrode preparation protocol and the amount of carbonaceous material incorporated onto the electrodic support was also an important factor studied. In this sense, CPE was modified adding different percentages of material to the paste, from 2.5 to 10%; the authors observed an increase of the oxidation peak of 4-chlorophenol for the electrodes with the highest amount of carbon material.

2.2 Ordered mesoporous carbons

The ordered mesoporous carbons (OMC) are nanostructured materials with extremely well-ordered pore network, high total pore volume, high specific surface area, and tuneable pore sizes in the mesopore range. OMC can be prepared either through a hard-template method by filling the mesopores of silica template with an organic precursor, or by an organic-organic (*i.e.*, copolymer molecular array and carbon precursor) self-assembly soft-templated method.[84-87] OMC are formed by a large number of graphene fragments on the carbon surface forming open mesopore channels that favour the confinement of biomolecules. OMC can act as hosts enhancing the mass transfer and providing an amplified analyte-receptor interface for electrochemical applications[46, 88-91] (Table 2).

Table 2. Figures of merit of selected OMC used to the fabrication of carbon-based electrochemical sensors.

Material	Type of porosity	Analytes	Concentration range	LOD	Sample	Technique	Ref.
Templated carbon	OMC	NADH H_2O_2	Up to 0.80 mM Up to 2 mM	5.60 µM 0.95 µM	Synthetic samples	CV, amperometry	88
Templated carbon	OMC	Ascorbic acid Dopamine Uric acid	80-1400 µM 0.4-60 µM 10-70 µM	14 µM 0.28 µM 1.6 µM	Human urine	DPV	90
Template-free carbon	OMC	Ascorbic acid Dopamine Uric acid	1.0-120.0 µM 0.05-14.50 µM 2.0-30.0 µM	0.10 µM 0.02 µM 0.14 µM	Urine	CV, SWV	91
Templated carbon	OMC	Amoxicillin	0.02-5 µM 0.005-1 µM	6 nM 1.5 nM	Tablets, human blood	LSV SW-AdASV	92
Oxidized commercial mesoporous carbon	OMC	Glucose	n.r.	n.r.	Synthetic samples	CV	78
Templated carbon	OMC	Amitrole	0.02- 0.25 mM	0.007 mM	River water	DPV	93
Templated carbon	OMC	Tryptophan	(0.5-70), (70-200) µM	0.035 µM	Synthetic samples	CV	94
Soft templated carbon	OMC	Norepinephrine	up to 500 pg/mL	100 pg/mL	Rabbit blood	Amperometry	95
CMK-3	OMC	Trans-resveratrol	5-50 µM	0.473 µM	Red wine	Amperometry	96
Carbon spheres	OMC	K^+	1 µM -1024 mM	5.4 µM	Synthetic samples	Potentiometry	98
Commercially mesoporous carbon	OMC	NO_3^-	1 -8 µM 8-800 µM	0.4 µM	Mineral water	Coulometry	99

n.r.: non-reported

Abdel-Galeil *et al.*[92] prepared a CPE, for the determination of amoxicillin, modified by two types of mesoporous carbons (named by the authors as MC and MC^-), MC prepared using SBA-15 as a hard-template and sucrose as carbon source, and MC^- synthesized using polyethylene-polypropylene glycol as a soft-template and resorcinol as carbon source. The results showed that the electrode modified with MC exhibited a higher peak current intensity associated to the acceleration of electron transfer process attributed to: (i) the greater conductivity and (ii) the adsorption of the analyte at carbon surface due to its highest surface area (1421 m^2/g) compared with MC^- sample (156 m^2/g). The preconcentration step improved the signal-to-background ratio rendering a simple, selective and reliable modified CPE sensor using linear sweep voltammetry (LSV) and square wave adsorptive anodic stripping voltammetry (SW-AdASV) techniques.

It is known that the functionalization of OMC could increase the density of active sites improving the sensor response and

also facilitating the simultaneous detection of analytes.[46, 78, 93, 94] In this regard, Lv and co-workers compared the response of glucose oxidase electrode using a pristine OMC and functionalized OMC on its manufacture.[78] This work reveals that the amount of fixed enzyme and its activity in carboxylated OMC is higher compared with pristine OMC. The enhanced enzyme adsorption is associated to the binding affinity of the oxygen containing groups on the surface of the functionalized OMC, while the higher activity may be linked to the presence of hydrophilic and ionic groups that facilitate the interactions between the COOH groups of the OMC and NH_2 groups on the GOD surface (Figure 4a).

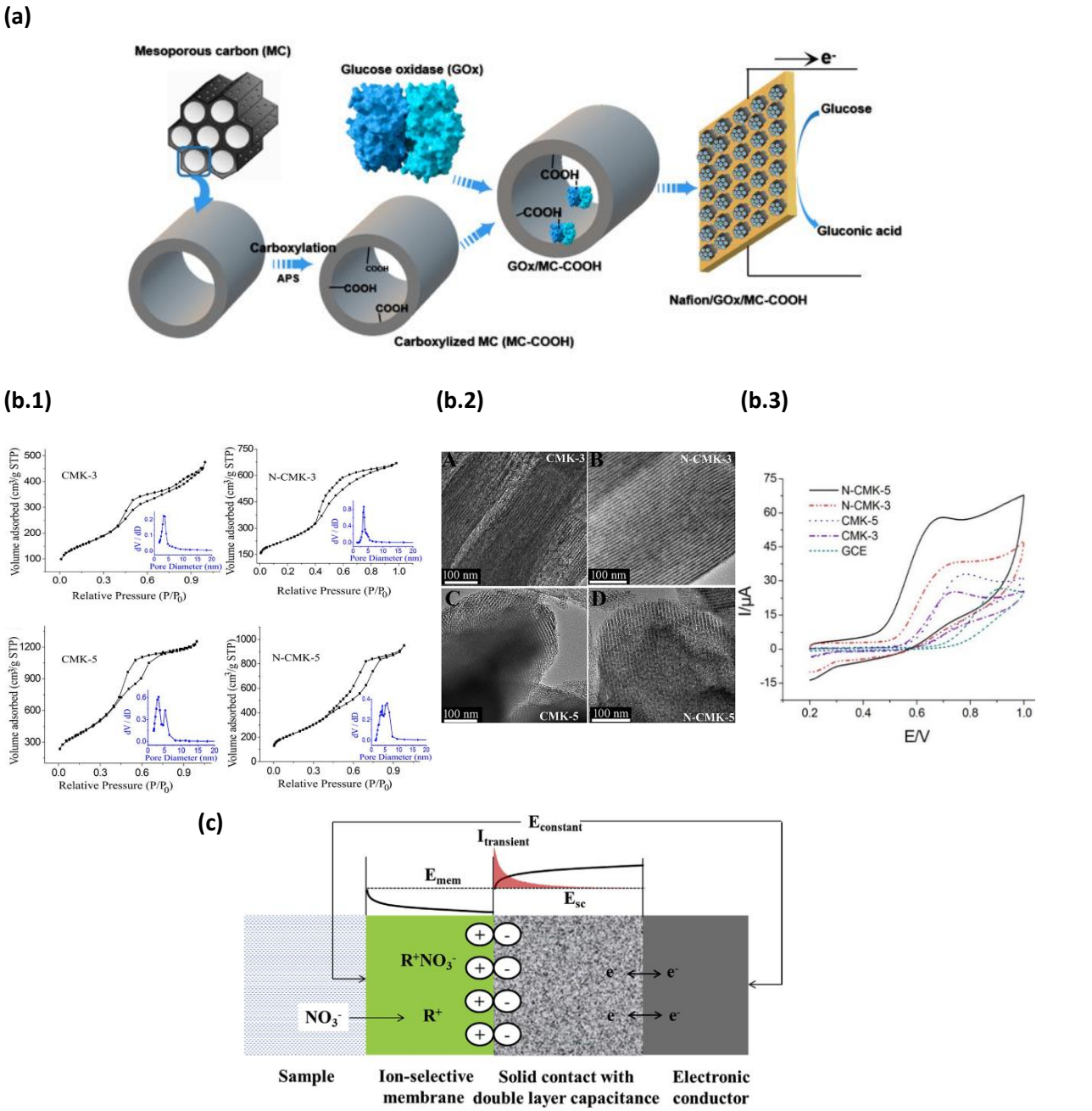

Fig. 4. (a) Scheme of functionalized mesoporous carbon preparation, enzyme immobilization and sensing mechanism (reproduced from ref. 78). **(b.1)** N_2 adsorption/desorption isotherms at 77 K of CMK-3, N-CMK-3, CMK-5 and N CMK-5 with pore size distributions inset; **(b.2)** TEM images of the four materials, and **(b.3)** cyclic voltammograms obtained in $Fe(CN)_6^{3-/4-}$ at GCE and modified GCE. Reprinted from ref. 93, Copyright 2021, with permission from Elsevier. **(c)** Scheme of the mechanism for the coulometric nitrate detection by SC-ISE constructed with OMC acting as solid-contact. Reprinted from ref. 99, Copyright 2020, with permission from Elsevier.

Zhou and co-workers reported the effect of nitrogen doped OMC modified sensor on the detection of a pesticide (amitrole).[93] They tested four OMC (named CMK-3, N-CMK-3, CMK-5 and N-CMK-5), all of them synthesized using SBA-15 as template. The materials showed different porous structure (Figure 4b.1) and N content, being the samples CMK-5 and N-CMK-5 with bimodal pore structure, the carbons with highest surface areas (1571 and 992 m^2/g, respectively). Consequently, the GCE modified with N-CMK-5 displayed the greatest oxidation peak of amitrole at smallest potential mainly associated to the large surface area, open pore structure, good conductivity and many edge-plane active sites (Figure 4b.1-2). Additionally, those materials doped with nitrogen (N-CMK-3 and N-CMK-5) presented larger response compared with their counterparts (Figure 4b.3), pointing out the improvement of electrochemical performance caused by the nitrogen content. The best tested material rendered a selective and sensitive sensor towards pesticide oxidation in the range of 0.02 to 0.25 mM. Zhou and collaborators also explored the role of nitrogen by constructing a nitrogen-doped OMC/Nafion/GCE sensor towards tryptophan.[94] The presence of doped OMC enhanced the electron and mass transfer at the electrode while the Nafion enabled the proton transfer, providing a sensor with wide linear concentration range and high selectivity.

With respect to the use of SPE, Dai and co-workers explored the preparation of an OMC-based SPE for the detection of norepinephrine (a neurotransmitter).[95] They fabricated an enzymatic sensor spreading, on a commercial SPE, the carbon ink consisting on OMC and poly(hydroxybutyl methacrylate) (as binder) dispersed in ethanol. For the amperometric measurements, a mixture of cofactor/enzyme/mediator was employed. The authors reported that an increase in both, surface area and pore size (until 6.5 nm), improves the sensitivity of the sensor associated with the adsorption of the enzyme and cofactor. Additionally, the authors conclude that the presence of microporous structure in the utilized carbons allows the adsorption of the mediator facilitating the charge transfer and enhancing the sensor response. On other research, a SPE was modified with a commercial OMC and Nafion film for the quantification of trans-resveratrol (poly-phenolic phytoalexin present in red wines).[96] Thanks to the abundant active sites for the analyte oxidation, caused by the high specific surface area (829 m^2/g) and carbon structure, the authors reported a good performance of the sensor with a linear response between 5 and 50 µM. However, for its application to real samples an extraction step is required and further improvements are needed to reach a fast determination in complex matrixes.

OMC have been also employed for the fabrication of solid-contact ion-selective electrodes (SC-ISEs). In these sensors, the carbonaceous material acts as ion-to-electron transducer layer (solid-contact) between the ion-selective membrane (ISM) and the conductive components.[97] Jiang *et al.* reported a K^+ selective electrode using OMC uniform spheres, obtained from a hydrothermal route, as solid contact.[98] The electrode was fabricated adding a dispersion of the OMC spheres onto a GCE, above this layer, a potassium ISM was drop-casted. The SC-ISE demonstrated a near-Nernstian response slope in the range of 0.001-1024 mM. The good performance of the sensor including high sensitivity, short response time (8 s), and good stability was mainly attributed to the high conductivity and capacitance of the OMC spheres that allow to stabilize the interfacial potentials within the electrode. Following with this type of configuration, Wang and co-workers investigated the use of commercial OMC as transducer on a SC-ISE for coulometric nitrate detection.[99] The authors reported suitable nitrate quantification with reproducible responses related to the high electrical power of OMC acting as electrochemical double-layer supercapacitor (Figure 4c). However, long time was required (more than 500 s) for the stabilization of the current-time curve.

2.3 Graphene-based materials

Graphene is comprised of a single layer of carbon atoms hexagonally arranged sp^2 bond network. This highly ordered crystalline structure endows this nanomaterial a great electrical conductivity. However, the complexity and cost to synthetize pure graphene in relatively high amounts have made that the graphene-based materials, such as graphene oxide (GO) or reduced graphene oxide (rGO), gain widespread consideration in several applications since they reach a compromise between the properties of graphene and the synthesis issues.

Porous graphene-based materials have been introduced to fully utilize the graphene intrinsic characteristics and high surface area since the presence of nanopores enhances their performance for several applications.[100, 101] Particularly, in sensing (Table 3), the perforation of graphene can play a paramount role in improving the electroactivity, as the additional channels promote ion and mass transport. Additionally, the pores on the graphene sheets produce extrinsic active sites with unsaturated carbon edges that can participate in the adsorption of the analytes. In the light of the above, the porous graphene-based materials have been employed on sensor platforms for the quantification of several analytes, including the porous graphene-based materials and composites porous graphene/functional materials.[101-107]

Liu and co-workers reported the synthesis of a graphene foam obtained by carbonization of a mixture of graphene oxide slurry and a prepared egg albumen foam. The material obtained was a N, S and Si co-doped graphene foam with a 3D structure.[108] The material showed an specific surface area of 1020 m^2/g with presence of mesopores centered at 4 nm of diameter, this porous network provided channels for fast ion and electron transfer allowing a large detection ranges. They modified a GCE with a graphene foam dispersion on polytetrafluoroethylene (PTFE) solution and evidenced the

quantification of dopamine in the range of 1.25 to 70 µM by DPV.

On other work, a porous graphene was synthetized using copper as an etching agent; after the elimination of copper, a graphene nanosheet (named P-GR) with a mesoporous structure was obtained (Figure 5a.1).[109] The material was casted on GCE surface and the modified electrode was employed as biosensor platform. The porous graphene modified sensor (P-GR/GCE) revealed better electrochemical responses compared with GCE, pyrolytic graphite electrode (PGE) and non-porous graphene modified electrode (GR/GCE) towards different compounds, being the improvement more remarkable for the detection of H_2O_2 and β-nicotinamide adenine dinucleotide (NADH) (Figure 5a.2-a.3). The greater performance of the porous electrode was mainly associated to its pore structure and higher amount of edge defect sites that provide more favourable sites which accelerate the electron-transfer kinetics.

Table 3. Figures of merit of the use of some graphene-based materials on the construction of electrochemical sensors.

Material	Type of porosity	Analytes	Concentration range	LOD	Sample	Technique	Ref.
GO	n.r.	Cardiac troponin-I	0.1-10 ng/mL	0.07 ng/mL	Clinical samples	CV	102
GO	n.r.	Carbaryl	0.3-6.1 ng/mL	0.15 ng/mL	Cabbage, spinach	DPV	105
Graphene frameworks	Micro-, mesoporous	H_2O_2	(0.196-22.34), (22.34-228.14), (228.14-11110) µM	0.032 µM	Synthetic samples	Amperometry	106
Graphene foam	Mesoporous	Dopamine	1.25-70 µM	1.25 µM	Synthetic samples	DPV	108
Graphene nanosheet	Mesoporous	H_2O_2 NADH	Up to 4 mM Up to 0.5 mM	1.94 µM 0.53 µM	Synthetic samples	Amperometry	109
3D graphene aerogel	n.r.	Glucose	1-18 mM	0.87 mM	Human serum	Amperometry	80
3D rGO hydrogel	Mesoporous	K^+	0.06-250 mM	0.06 mM	Sport drinks	Potentiometry	110
Graphene	Micro/ nanoporous	K^+	0.01-100 mM	7 µM	Artificial sweat	Potentiometry	111
LIG	n.r	Trans-resveratrol	0.2-50 µM	0.16 µM	Red wine	DPV	115
LIG	Micro-, mesoporous	Hydrazine	0.1-0.5 mM	70 µM	Synthetic samples	CV	116
LIG	Macroporous	miRNA	n.r.	10 fM*	Synthetic samples	DPV	117
LIG	n.r.	Uric acid Tyrosine	3.50 µA μM^{-1} cm^{-2} * 0.61 µA μM^{-1} cm^{-2} *	0.75 µM 3.6 µM	Sweat	DPV	118
LIG	Mesoporous	COVID-19	n.r.	n.r.	Blood, saliva	Amperometry	119

*n.r.: non-reported; *sensitivity*

Interestingly, Xu and collaborators developed a microfluidic electrochemical biosensor for glucose detection.[80] They fabricated a chip through a microchannel bonded on ITO substrate in which a graphene hydrogel was synthetized by *in-situ* chemical reduction of GO followed by freeze-dried; the result was a microfluidic device (less than 3 µL of sample is needed) in which GOD is adsorbed, after 15 min of incubation, in the porous structure generated during the freeze drying step. Due to the protection of GOD and stability in the carbonaceous network, the sensor presented a good stability, sensitivity and selectivity, reporting a greater current response (chronoamperometry at -0.3 V) to glucose than uric acid, ascorbic acid, lactose, maltose, fructose and sucrose.

Reduced graphene oxide hydrogel with a relatively large surface area (247 m^2/g) and developed pore structure was prepared by a hydrothermal reduction of a graphene oxide solution.[110] The material was employed as ion-to-electron transducer to be applied to solid-contact potassium-selective electrodes, for that matter, the 3D rGO was drop-casted on Au substrate followed by ISM coverage. The rGO provides a high electrical double-layer capacitance that is essential for effective solid-contact transducers. Additionally, the hydrophobic character of the reduced material avoids the formation of a water layer of the SC-ISE surface, preventing the diffusion of undesired ions or gases and rendering stable potential responses of the sensor. The device showed a linear slope of 53.34 mV/log[K^+] which is close to a Nernstian behaviour. The porous rGO solid-contact-based electrode enhanced potential stability in a long period of time and gave a lower sensitivity towards light, oxygen and carbon dioxide, being a promising transducer for reliable electrochemical performance of SC-ISE. In this regard, He and collaborators constructed a graphene-based SC-ISE for K^+ sensing by inkjet printing process (Figure 5b.1),[111] the annealing of printed graphite at 950 °C in nitrogen atmosphere improved the electrical conductivity and generated a connected porous structure which, after modification with a potassium ionophore, displayed a sensor with low detection limit (7 µM)

and negligible interferences in sweat (Figure 5b.2). Recently, CO_2 laser was employed to synthesize the known laser induced graphene (LIG) from polyimide film rendering a graphene with high electrical conductivity and large surface area (usually *ca.* 340 m^2/g).[112] LIG, due to its 3D architecture enriched with edge planes and the simplicity of processing, is a promising material for sensing applications.[113-116] In this kind of devices, the graphene is not purely a modifier, since the carbonaceous material is directly engraved on the source (polyimide flexible support) generating the electrodic surface.

Figure 5c shows the fabrication process of biosensor for miRNA based on LIG.[117] The authors characterized the LIG electrode by Raman spectroscopy, revealing the ability to module the I_D/I_G ratio (material order) by the characteristics of employed laser. Additionally, they reported the control of N-doping in the graphene skeleton. The purified miRNA was drop-casted onto the LIG electrode to be adsorbed on the porosity (macropores) of the generated graphene-like material, then an electrochemical test in the presence of redox pair was carried out. The presence of N-graphitic and the porous structure improved the resistance and affinity with nucleic acids allowing the detection of miRNA with 10 fM of sensitivity.

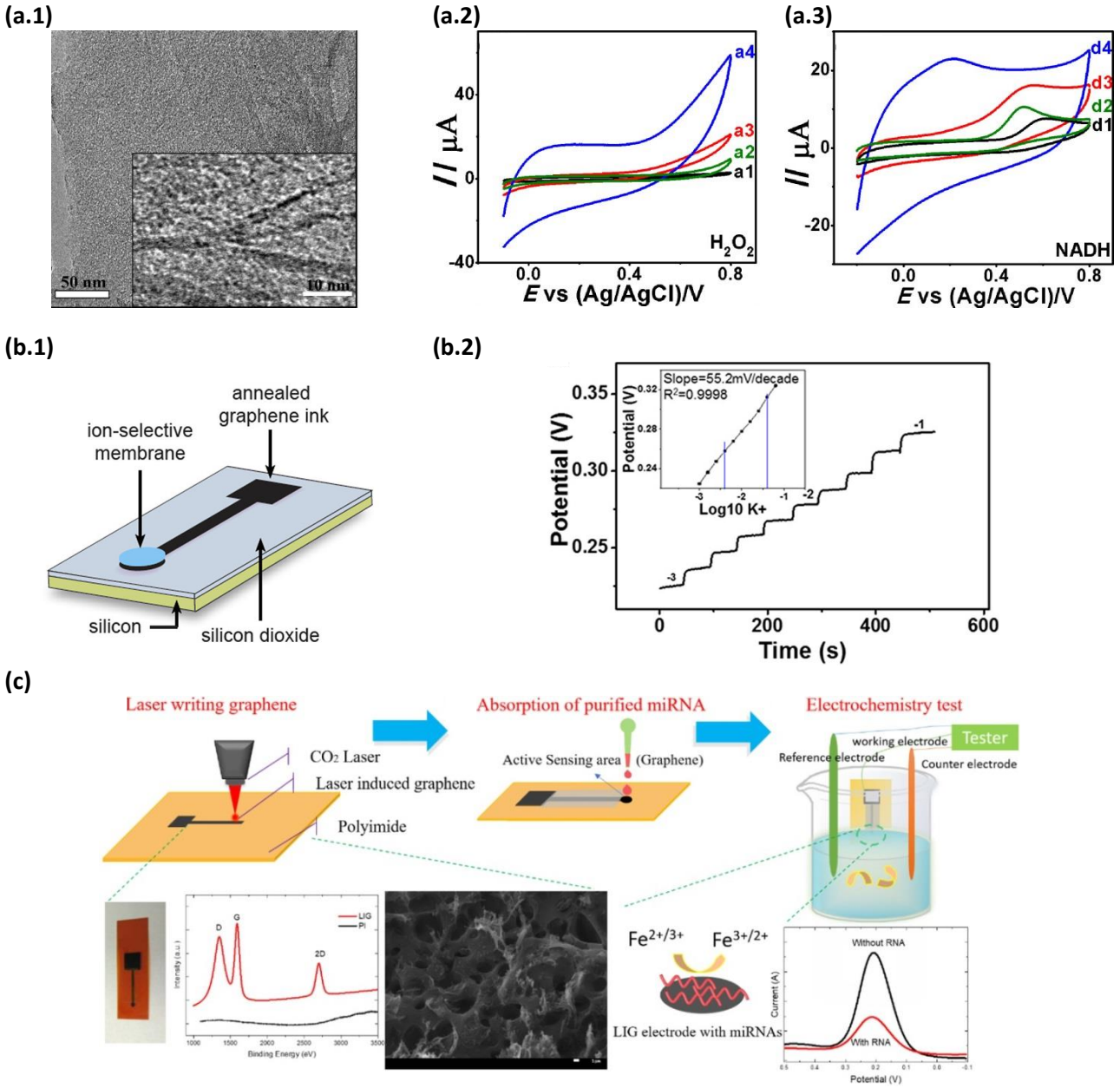

Fig. 5. (a.1) TEM image of P-GR, **(a.2)** CV of 8 mM H_2O_2 recorded on GCE (a1), PGE (a2), GR/GCE (a3), and P-GR/GCE (a4), and **(a.3)** 2 mM NADH recorded on GCE (d1), PGE (d2), GR/GCE (d3), and P-GR/GCE (d4). Reprinted from ref. 109, Copyright 2014, with permission from Elsevier. **(b.1)** Scheme of SC-ISM integration on the annealed graphene electrode, **(b.2)** K^+ calibration plot for SC-ISE electrode in sweat. Reprinted with permission from ref. 111. Copyright 2017 American Chemical Society. **(c)** Schematic synthesis and application of miRNA LIG-based biosensor. The Raman spectra of the LIG and the SEM image with scale bar of 1 µm are included (reprinted from ref. 117, Copyright 2020, with permission from Elsevier).

Yang *et al.* reported the use of three electrode LIG-based chemical sensor to detect uric acid and tyrosine by DPV on sweat samples *in-situ*.[118] The authors stated that the accurate and rapid detection of both analytes, and superior electrochemical performance over glassy carbon, screen-printed carbon and gold electrodes was ascribed to the fast electron mobility and high current density provided by the graphene.

Most recently, a graphene-based electrode was reported for COVID-19 diagnosis and monitoring.[119] The approach consisted on the immobilization of antigens and antibodies on the four functionalized LIG mesoporous electrodes. The combination of the properties of graphene and the immunosensing strategy allowed the development of sensor with high sensitivity and specificity.

2.4 MOF-derived carbon materials

MOFs are a class of crystalline porous materials assembled of metal ions or clusters linked by organic ligands via coordination bonds. The characteristics of these porous networks entail large specific surface areas and well-defined pore size distributions, as well as controllable chemical functionalization at the surface.[120] Although various reports describe the use of MOFs to fabricate electrochemical sensors,[121-124] it is difficult to use them for an efficient electrochemical performance due to the instability in water of most of them and their poor electrical conductivity.[125] In this sense, through thermal treatment under an inert atmosphere, the polymeric organic structure becomes carbonaceous material, remaining the framework of the pristine MOFs and their features in terms of electrical conductivity will be considerably improved, which opens up possibilities for chemical separations, environmental remediation, ion exchange, (photo)catalysis and sensing.[126-128] In this regard, various works have been published during the last decade reporting the use of MOF-derived carbon materials as modifiers of electrodes to enhance the sensing performance towards different analytes[129-133] (Table 4).

Table 4. Figures of merit of the use of MOF-derived carbon materials for electrochemical sensing.

Material	Type of porosity	Analytes	Concentration range	LOD	Sample	Technique	Ref.
MOF-derived	Micro-, mesoporous	Cd^{2+}	0.025–5 μM	2.2 nM	Tap water, lake water	SWASV	129
MOF-derived	Microporous	Uric acid Hydroquinone Catechol	1-300 μM 1-200 μM 1-300 μM	0.014 μM 0.348 μM 0.267 μM	Human serum	DPV	130
MOF-derived	Micro-, mesoporous	Metronidazole	0.05-100 μM	17 nM	Pharmaceuticals	LSV	131
MOF-derived	Meso-, macroporous	Quercetin	(0.2-10), (10-200) μM	83.3 nM	Flos Sophora	DPV	132
MOF-derived	Microporous	Chloramphenicol	(0.05-100) μM, (0.10-3) mM	0.04 μM	Honey, milk, domestic sewage	SWV	133
MOF-derived	Micro-, mesoporous	Hydroquinone Catechol	1-70 μM 1-100 μM	0.18 μM 0.31 μM	Local water	DPV	134
MOF-derived	Mesoporous	Hydroquinone Catechol	1-120 μM 1-200 μM	1 μM 1 μM	River water	DPV	135
MOF-derived	Micro-, macroporous	Quercetin	0.1-20 μM 20-120 μM	0.03 μM	Ginkgo biloba extract tablet	DPV	136
MOF-derived	Micro-, mesoporous	Uric acid	2-110 μM	0.83 μM	Human serum	DPV	137
MOF-derived	Micro-, mesoporous	Chloramphenicol	0.01-1 μM 1-4 μM	0.0029 μM	Honey	SWV	138
MOF-derived	Micro-, mesoporous	Lidocaine	0.0002-8 μM	0.00006 μM	Rat serum	CV	139

A simultaneous determination of hydroquinone and catechol was explored by a MOF-derived nanoporous carbon modified glassy carbon electrode.[134] Two porous materials, obtained by the carbonization of two isomorphic MOFs formed by the coordination between zinc ion and a ligand (FJU-40-H and FJU-40-NH_2) were tested. The presence of the ligands rendered two different carbon materials in terms of porosity, while FJU-40-H produced a mesoporous material with a high surface area (1242 m^2/g), FJU-40-NH_2 was become microporous carbon with a lower surface area (592 m^2/g), pointing out the influence of the ligand on the final material. The performance of modified sensor towards hydroquinone and catechol oxidation revealed that only the carbonaceous material synthesized from FJU-40-H allowed the determination of these molecules. The authors address this achievement to the fact of the structure loss, the higher porosity and the micro-mesoporous character of that material, which could be beneficial to the dispersion of the other components and thereby improving the catalytic activity. Furthermore, the good conductivity and the greater N-graphitic content can be attributed to the better sensing performance. In this regard, Zhang *et al.* studied the role of the carbon materials

N content.[135] They synthesized a series of carbon materials by one-step carbonization of ZIF-67/PAN nanofibers composite at different temperatures (Figure 6a). The authors concluded that a synergistic effect between the porosity and N content promotes the electrochemical performance of the modified-GCE, being the electrode modified with the material with higher N content (6.33%) and large specific surface area (350 m^2/g) the most sensitive for the simultaneous determination of hydroquinone and catechol by DPV.

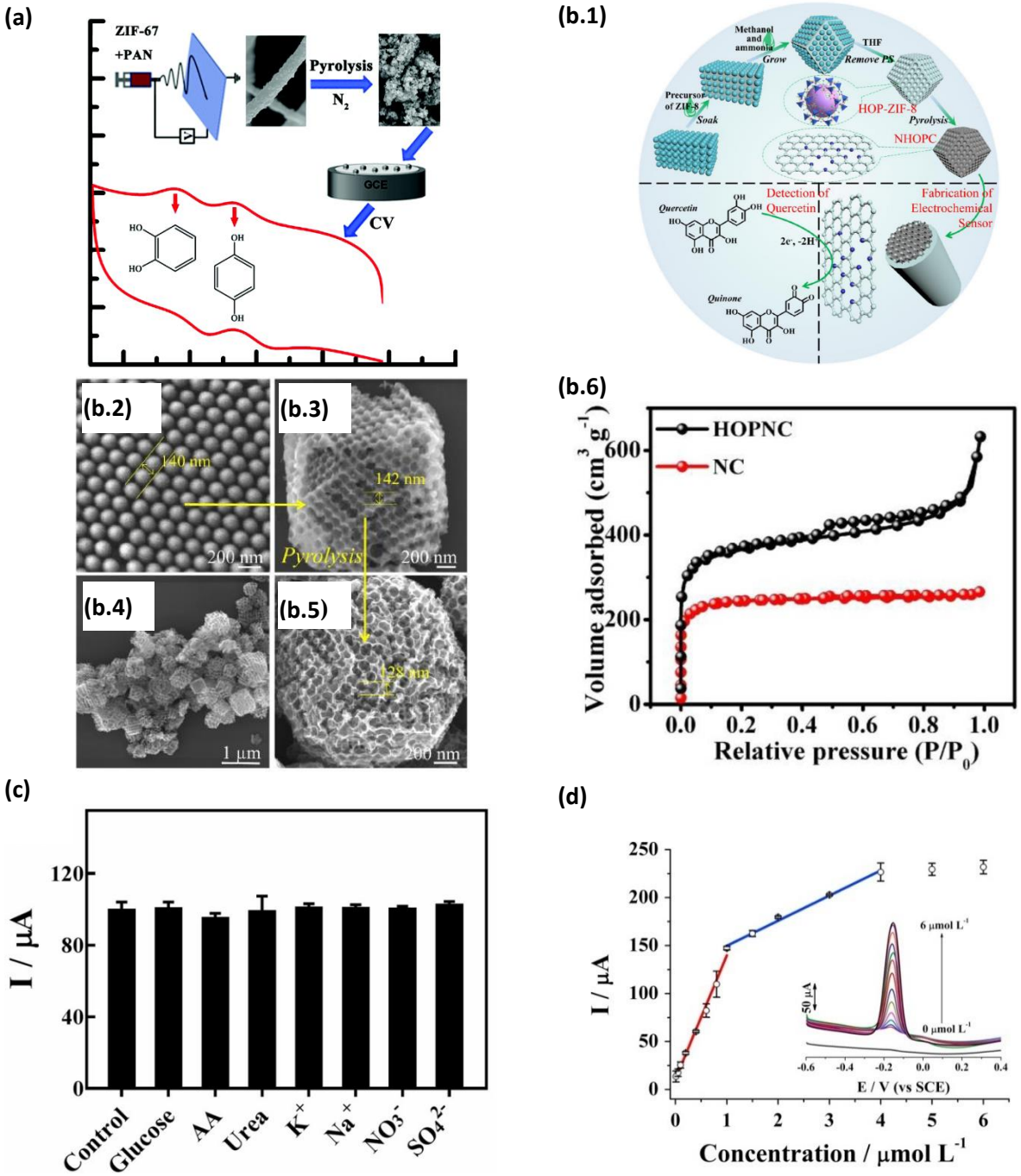

Fig. 6. (a) Synthesis process of carbon-ZIF-67/PAN obtained by carbonization at 800 °C and the application of modified-electrode. Reproduced from ref. 135. **(b.1)** Scheme of HOPNC synthesis and oxidation mechanism of quercetin on modified GCE. SEM images of **(b.2)** PS template, **(b.3)** hierarchically ordered ZIF-8 and **(b.4-5)** HOPNC. **(b.6)** N_2 adsorption-desorption isotherms at 77 K of NC and HOPNC. Reprinted from ref. 136 Copyright 2020, with permission from Elsevier. **(c)** Current obtained in 50 µM uric acid on modified-electrode with the presence and absence of 5 mM interferents in 0.1 M PBS (pH 7). Reprinted from ref. 137, Copyright 2019, with permission from Elsevier. **(d)** SWV response of modified electrode in 0.1 M PBS (pH 5.5) with different concentration of chloramphenicol by 180 s of accumulation on open circuit and plot of current peaks *vs.* concentration. Reprinted from ref. 138, Copyright 2017, with permission from Elsevier.

Lately, a hierarchically ordered porous nitrogen doped carbon (HOPNC) was employed to modify a GCE for the quantification of quercetin (a flavonoid).[136] The authors used polystyrene microspheres (PS) as template to synthesize a hierarchically ordered porous ZIF-8, which subsequently was carbonized to obtain the HOPNC (Figure 6b.1). SEM images showed the 3D-ordered macroporous -with a diameter of 142 nm (close to PS template's size)- and microporous structure of the synthetized ZIF-8 (Figure 6b.2-3). Then, after the carbonization step a large number of defects were formed (Figure 6b.4-5). The larger surface area (958 m^2/g) of the HOPNC compared with the conventional ZIF-8 carbonization product (NC) is attributed to the interconnected meso/macroporous structure (Figure 6b.6). That structure, along with the nitrogen content, provokes an enhanced activity of HOPNC/GCE due to (i) improved contact surface area and more adsorption sites for target molecule, (ii) acceleration of mass transfer of quercentin and ions, and (iii) ameliorated affinity between carbon and quercetin. The authors reported a good selectivity, repeatability (relative standard deviations of 1.2 % after 5 times) and sensitivity for the modified electrode with a LOD of 0.03 µM towards the flavonoid.

Liu and co-workers[137] have published the direct carbonization of BMZIF nanocrystals (bimetallic zeolitic imidazolate frameworks, based on ZIF-8 and ZIF-67) to obtain a N,Co-co-doped porous carbon. They casted a suspension of the obtained material on a GCE and employed it for the detection of uric acid by DPV. Their results pointed out the good electrochemical activity of the fabricated sensor due to the relatively high porosity of the material, facilitating the oxidation of the uric acid on the electrode surface and therefore increasing the response of the sensor. Additionally, the anti-interference ability was demonstrated towards most common molecules present in real samples (Figure 6c).

On other research, an exfoliated carbon material obtained by sonication (in N-methylpyrrolidone) of carbonized IRMOF-8 was employed to modify a GCE.[138] The authors reported a higher sensitivity, towards the detection of chloramphenicol (an antibiotic), for the exfoliated carbon-modified GCE compared to its parental non-exfoliated carbon-modified electrode (Figure 6d). This fact was associated with the slightly superior surface area (1854 *vs.* 1336 m^2/g, respectively) and, more remarkable, higher dispersibility in N,N-dimethylformamide of the exfoliated material facilitating the homogeneous modification of the electrode.

In 2018, a hybrid sensor for a selective detection of lidocaine was reported.[139] The authors modified a GCE by casting a dispersion of porous carbon, obtained from the carbonization at 1000 °C of IRMOF-8. Then, a layer of a molecularly imprinted polymer (MIP) was *in-situ* deposited followed by the elimination of the used templated (resorcinol); this layer acted as a target molecule recognizer. Moreover, the porous carbon improves the conductivity and provides a greater loading surface for the MIP; on the other, the MIP layer allows the selective recognition of lidocaine. As a result, the authors propose a highly sensitive and selective sensor that enables the determination of the anesthesic concentration with the order of pM. However, the laborious fabrication of the sensor, and the long incubation period required to led the target molecules occupy the imprinted sites make the device impractical to the real application.

3 Conclusions and perspectives

Inherent attributes when using porous carbon materials, in terms of high surface area and tuneable structure and surface chemistry, may offer important and crucial electrochemical advantages mainly associated to the enhancement of electron transfer kinetics in electrochemical sensing applications. During the last years, research efforts have aimed to improve the performance of (bio)electrochemical sensing devices through simple methodologies consisted of modifying underlying substrates commonly used in electrochemistry. In this review, we have illustrated and described the synthesis of a series of porous carbons (*i.e.*, activated carbons, ordered mesoporous carbons, graphene based-materials and MOF-derived carbons), analysing its properties. A summary of the main features, advantages and limitations of the mentioned materials is collected in Table 5. Additionally, we have discussed its incorporation onto GCE, carbon paper or screen-printed electrodes, among others, exhibiting high sensitivity, wide linear range concentration, and low LOD towards a wide variety of molecules of interest.

Table 5. Summary of the main properties, advantages and limitations of the four porous carbon materials described in this review. The features are described as a general trend.

Material	Structure/Porosity	Main advantages	Limitations
Activated Carbon	Disordered/High	Cost-effective precursors	Uncontrolled porosity
OMC	Ordered/High-Medium	Controlled porosity	Expensive/laborious synthesis
Graphene-based	Ordered/Medium-Low	High conductivity	Limited porosity and expensive/laborious synthesis
MOF-derived	Ordered/High-Medium	Controlled porosity	Expensive/laborious synthesis

Even though a huge progress has been reached regarding the carbonaceous ink preparation and design of methodologies for the modification of conductive substrates, where most of them are now well-established in the benchmark laboratory, challenges are still on the table and opened up for discussion for further development and applicability. Accordingly, scaling of the simplest, low-cost and mass produced tailored syntheses of porous carbons with defined textural, structural and surface chemistry is the need of the hour towards green and smart electrosensing devices (adapting the features and manufacture of the material to the target analyte). The reformulation of porous carbon-based inks for the development of electrochemical sensor platforms in 2D and 3D polymeric structures has to be also faced on; similarly, strategies for the use of porous carbons in screen printing, ink printing or 3D printing are also mandatory for manufacture and deployment for the portability use and *in-situ* applications. Another major issue, which is not treated in this review, is the use of porous carbon in the development of the electrochemical sensing of gases, so the monitoring and quantification of hazardous gases provides a wide number of opportunities for research and this represents a huge niche market for enterprises and public health sector. Finally, more progress on the preparation of different structures of porous carbon materials for the electrochemical sensing therefore does not need to leave behind of nowadays call in sensing or another fields related to electrochemistry; in this regard, carbon quantum dots or carbon nitrides are quite few examples which deserves to be tried and compared in the near future.

Author Contributions

Conceptualization, A.C., J.I. and A.G.-B.; investigation, A.C. and A.G.-B.; writing—original draft preparation, A.C. and A.G.-B.; writing—review and editing, A.C., J.I. and A.G.-B. All authors have read and agreed to the published version of the manuscript.

Conflicts of interest

There are no conflicts to declare.

Acknowledgements

A.C. gratefully thanks KTH Royal Institute of Technology. J.I. thanks Spanish MINICINN (PID2019-108136RB-C32) for its financial support. A.G-B. thanks European Union-NextGenerationEU (ZAMBRANO21-10) for the funding.

Notes and references

1. J. Iniesta, L. García-Cruz, A. Gomis-Berenguer and C. O. Ania, in *Electrochemistry*, eds. C. E. Banks, R. Mortimer and S. McIntosh, Royal Society of Chemistry, United Kingdom, 2016, vol. 13, pp. 133-165.
2. *Nanocarbon electrochemistry*, John Wiley, Sussex, United Kingdom, 2020.
3. J. Wang, *Electroanalysis*, 2005, **17**, 7-14.
4. C. E. Banks and R. G. Compton, *Analyst*, 2006, **131**, 15-21.
5. C. Yang, M. E. Denno, P. Pyakurel and B. J. Venton, *Analytica Chimica Acta*, 2015, **887**, 17-37.
6. A. Sanati, M. Jalali, K. Raeissi, F. Karimzadeh, M. Kharaziha, S. S. Mahshid and S. Mahshid, *Microchimica Acta*, 2019, **186**, 22.
7. S. G. A. Hulanicki, F. Ingman, *Pure & Appl. Chem.* , 1991, **63**, 1247.
8. J. Bobacka, *Journal of Solid State Electrochemistry*, 2020, **24**, 2039-2040.
9. R. N. Adams, *Analytical Chemistry*, 1958, **30**, 1576-1576.
10. P. J. Britto, K. S. V. Santhanam and P. M. Ajayan, *Bioelectrochemistry and Bioenergetics*, 1996, **41**, 121-125.
11. F. Patolsky, G. Tao, E. Katz and I. Willner, *Journal of Electroanalytical Chemistry*, 1998, **454**, 9-13.
12. X. Dang, C. Hu, Y. Wei, W. Chen and S. Hu, *Electroanalysis*, 2004, **16**, 1949-1955.
13. V. Vamvakaki, K. Tsagaraki and N. Chaniotakis, *Analytical Chemistry*, 2006, **78**, 5538-5542.
14. S. E. Baker, P. E. Colavita, K. Y. Tse and R. J. Hamers, *Chemistry of Materials*, 2006, **18**, 4415-4422.
15. N. Jia, Z. Wang, G. Yang, H. Shen and L. Zhu, *Electrochemistry Communications*, 2007, **9**, 233-238.
16. S. Alwarappan, A. Erdem, C. Liu and C. Z. Li, *Journal of Physical Chemistry C*, 2009, **113**, 8853-8857.
17. C. Shan, H. Yang, J. Song, D. Han, A. Ivaska and L. Niu, *Analytical Chemistry*, 2009, **81**, 2378-2382.
18. P. Gai, H. Zhang, Y. Zhang, W. Liu, G. Zhu, X. Zhang and J. Chen, *Journal of Materials Chemistry B*, 2013, **1**, 2742-2749.
19. A. Walcarius, *Electroanalysis*, 2015, **27**, 1303-1340.
20. M. Thommes, K. Kaneko, A. V. Neimark, J. P. Olivier, F. Rodriguez-Reinoso, J. Rouquerol and K. S. W. Sing, *Pure and Applied Chemistry*, 2015, **87**, 1051-1069.
21. F. R. R. Teles and L. P. Fonseca, *Materials Science and Engineering: C*, 2008, **28**, 1530-1543.
22. D. Yildirim, D. Alagöz, A. Toprak, S. Tükel and R. Fernandez-Lafuente, *Process Biochemistry*, 2019, **85**, 97-105.
23. Z. S. Aghamiri, M. Mohsennia and H. A. Rafiee-Pour, *Talanta*, 2018, **176**, 195-207.
24. A. G. Pandolfo and A. F. Hollenkamp, *Journal of Power Sources*, 2006, **157**, 11-27.
25. *Carbons for electrochemical energy storage and conversion systems*, CRC Press, Boca Raton, Florida, USA, 1st edn., 2009.
26. C. González-Gaitán, R. Ruiz-Rosas, E. Morallón and D. Cazorla-Amorós, *International Journal of Hydrogen Energy*, 2015, **40**, 11242-11253.
27. W. Li, M. Seredych, E. Rodríguez-Castellón and T. J. Bandosz, *ChemSusChem*, 2016, **9**, 606-616.
28. J. L. Figueiredo, *Journal of Materials Chemistry A*, 2013, **1**, 9351-9364.
29. N. M. Bardhan, *Journal of Materials Research*, 2017, **32**, 107-127.

30. L. Nayak, M. Rahaman and R. Giri, in *Carbon-containing polymer composites*, eds. M. Rahaman, D. Khastgir and A. K. Aldalbahi, Springer Series, Singapore, 2019, DOI: 10.1007/978-981-13-2688-2, ch. 2.
31. W. Putzbach and N. Ronkainen, *Sensors*, 2013, **13**, 4811-4840.
32. M. Wei and S. Feng, *Microchimica Acta*, 2017, **184**, 3461-3468.
33. S. Mutyala, J. Kinsly, G. V. R. Sharma, S. Chinnathambi and M. Jayaraman, *Journal of Electroanalytical Chemistry*, 2018, **823**, 429-436.
34. M. Sivakumar, V. Veeramani, S. M. Chen, R. Madhu and S. B. Liu, *Microchimica Acta*, 2019, **186**, 59.
35. S. Dong, D. Zhang, H. Cui and T. Huang, *Sensors and Actuators B: Chemical*, 2019, **284**, 354-361.
36. X. Yang, P. Zhao, Z. Xie, M. Ni, C. Wang, P. Yang, Y. Xie and J. Fei, *Talanta*, 2021, **233**, 122545.
37. P. Veerakumar, V. Veeramani, S. M. Chen, R. Madhu and S. B. Liu, *ACS Applied Materials & Interfaces*, 2016, **8**, 1319-1326.
38. P. Niu, C. Fernández-Sánchez, M. Gich, C. Ayora and A. Roig, *Electrochimica Acta*, 2015, **165**, 155-161.
39. P. Veerakumar, A. Sangili, S.-M. Chen, A. Pandikumar and K.-C. Lin, *ACS Sustainable Chemistry & Engineering*, 2020, **8**, 3591-3605.
40. N. Gissawong, S. Srijaranai, S. Boonchiangma, P. Uppachai, K. Seehamart, S. Jantrasee, E. Moore and S. Mukdasai, *Microchimica Acta*, 2021, **188**, 208.
41. A. Bianco, Y. Chen, E. Frackowiak, M. Holzinger, N. Koratkar, V. Meunier, S. Mikhailovsky, M. Strano, J. M. D. Tascon and M. Terrones, *Carbon*, 2020, **161**, 373-391.
42. V. S. Bhat, S. S and G. Hegde, *Journal of The Electrochemical Society*, 2020, **167**, 037526.
43. A. Walcarius, S. D. Minteer, J. Wang, Y. Lin and A. Merkoci, *Journal of Materials Chemistry B*, 2013, **1**, 4878-4908.
44. I. Švancara, K. Kalcher, A. Walcarius and K. Vytřas, *Electroanalysis with carbon paste electrodes*, CRC Press, Boca Raton, Florida, USA, 1st edn., 2012.
45. I. Švancara, K. Vytřas, K. Kalcher, A. Walcarius and J. Wang, *Electroanalysis*, 2009, **21**, 7-28.
46. A. Walcarius, *Sensors* 2017, **17**, 42.
47. E. Nossol and A. J. G. Zarbin, *Electrochimica Acta*, 2008, **54**, 582-589.
48. J. P. Metters, R. O. Kadara and C. E. Banks, *Analyst*, 2011, **136**, 1067-1076.
49. A. Smart, A. Crew, R. Pemberton, G. Hughes, O. Doran and J. P. Hart, *Trends in Analytical Chemistry*, 2020, **127**, 115898.
50. D. D. Liana, B. Raguse, J. J. Gooding and E. Chow, *Sensors*, 2012, **12**, 11505-11526.
51. A. Sánchez-Calvo, E. Núñez-Bajo, M. T. Fernández-Abedul, M. C. Blanco-López and A. Costa García, *Electrochimica Acta*, 2018, **265**, 717-725.
52. J. Wang, Q. Chen, C. L. Renschler and C. White, *Analytical Chemistry*, 1994, **66**, 1988-1992.
53. Q. Cao and J. A. Rogers, *Advanced Materials*, 2009, **21**, 29-53.
54. D. Feng, Y. Lv, Z. Wu, Y. Dou, L. Han, Z. Sun, Y. Xia, G. Zheng and D. Zhao, *Journal American Chemical Society*, 2011, **133**, 15148-15156.
55. M. Sevilla and R. Mokaya, *Energy Environ. Sci.*, 2014, **7**, 1250-1280.
56. H. Marsh and F. Rodriguez-Reinoso, *Activated Carbon*, Elsevier, 2006.
57. *Carbon materials for catalysis* Wiley 2008.
58. *Activated carbon surfaces in environmental remediation*, Elsevier, 2006.
59. D. Spanu, G. Binda, C. Dossi and D. Monticelli, *Microchemical Journal*, 2020, **159**, 105506.
60. J. J. Arroyo-Gómez, D. Villarroel-Rocha, K. C. de Freitas-Araújo, C. A. Martínez-Huitle and K. Sapag, *Journal of Electroanalytical Chemistry*, 2018, **822**, 171-176.
61. J. Han, J. Zhao, Z. Li, H. Zhang, Y. Yan, D. Cao and G. Wang, *Journal of Electroanalytical Chemistry*, 2018, **818**, 149-156.
62. W. Zhang, L. Liu, Y. Li, D. Wang, H. Ma, H. Ren, Y. Shi, Y. Han and B. C. Ye, *Biosensors Bioelectronics*, 2018, **121**, 96-103.
63. B. Sun, D. Li, J. Cai, W. Li, X. Gou, Y. Gou and F. Hu, *Journal of The Electrochemical Society*, 2019, **166**, H33-H40.
64. V. Sudha, S. M. Senthil Kumar and R. Thangamuthu, *Colloids Surfaces B Biointerfaces*, 2019, **177**, 529-540.
65. F. Laghrib, H. Hammani, A. Farahi, S. Lahrich, A. Aboulkas and M. A. El Mhammedi, *Russian Journal of Electrochemistry*, 2021, **57**, 532-543.
66. H. Hammani, A. Hrioua, S. Aghris, S. Lahrich, S. Saqrane, M. Bakasse and M. A. El Mhammedi, *Materials Chemistry and Physics*, 2020, **240**, 122111.
67. P. R. de Oliveira, C. Kalinke, J. L. Gogola, A. S. Mangrich, L. H. Marcolino Junior and M. F. Bergamini, *Journal of Electroanalytical Chemistry*, 2017, **799**, 602-608.
68. C. Kalinke, A. S. Mangrich, L. H. Marcolino-Junior and M. F. Bergamini, *Electroanalysis*, 2016, **28**, 764-769.
69. R. Madhu, K. V. Sankar, S.-M. Chen and R. K. Selvan, *RSC Advances*, 2014, **4**, 1225-1233.
70. J. Guan, Y. Fang, T. Zhang, L. Wang, H. Zhu, M. Du and M. Zhang, *Electrocatalysis*, 2020, **11**, 59-67.
71. Y. Baikeli, X. Mamat, N. Yalikun, Y. Wang, M. Qiao, Y. Li and G. Hu, *RSC Advances*, 2019, **9**, 23678-23685.
72. Z. Lu, Y. Wang, Y. Hasebe and Z. Zhang, *Electroanalysis*, 2020, **33**, 956-963.
73. K. B. Akshaya, V. S. Bhat, A. Varghese, L. George and G. Hegde, *Journal of The Electrochemical Society*, 2019, **166**, B1097-B1106.
74. V. Veeramani, M. Sivakumar, S.-M. Chen, R. Madhu, H. R. Alamri, Z. A. Alothman, M. S. A. Hossain, C.-K. Chen, Y. Yamauchi, N. Miyamoto and K. C. W. Wu, *RSC Advances*, 2017, **7**, 45668-45675.
75. D. Kim, J. M. Kim, Y. Jeon, J. Lee, J. Oh, W. Hooch Antink, D. Kim and Y. Piao, *Sensors and Actuators B: Chemical*, 2018, **259**, 50-58.
76. J. Chen, R. Zhu, J. Huang, M. Zhang, H. Liu, M. Sun, L. Wang and Y. Song, *Analyst*, 2015, **140**, 5578-5584.
77. C. O. Ania, A. Gomis-Berenguer, J. Dentzer and C. Vix-Guterl, *Journal of Electroanalytical Chemistry*, 2018, **808**, 372-379.
78. C. Lv, S. Li, L. Liu, X. Zhu and X. Yang, *Sensors*, 2020, **20**, 3365.
79. A. F. Quintero-Jaime, J. Quílez-Bermejo, D. Cazorla-Amorós and E. Morallón, *Electrochimica Acta*, 2021, **367**.
80. J. Xu, K. Xu, Y. Han, D. Wang, X. Li, T. Hu, H. Yi and Z. Ni, *Analyst*, 2020, **145**, 5141-5147.

81. B. Shan, Y. Ji, Y. Zhong, L. Chen, S. Li, J. Zhang, L. Chen, X. Liu, Y. Chen, N. Yan and Y. Song, *RSC Advances*, 2019, **9**, 25647-25654.
82. K. D. Ramadhass, M. Ganesan, T.-W. Chen, S.-M. Chen, M. A. Ali, M. A. Habila, A. El-Marghany and M. Sheikh, *Journal of The Electrochemical Society*, 2021, **168**, 047503.
83. A. Deryło-Marczewska, K. Skrzypczyńska, K. Kuśmierek, A. Świątkowski and M. Zienkiewicz-Strzałka, *Adsorption*, 2019, **25**, 357-366.
84. R. Ryoo, S. H. Joo and S. Jun, *Physical Chemistry B*, 1999, **103**, 7743-7746.
85. S. Jun, S. H. Joo, R. Ryoo, M. Kruk, M. Jaroniec, Z. Liu, T. Ohsuma and O. Terasaki, *Journal American Chemical Society*, 2000, **122**, 10712-10713.
86. R. Ryoo, S. H. Joo, M. Kruk and M. Jaroniec, *Advanced Materials*, 2001, **13**, 677-681.
87. W. Xin and Y. Song, *RSC Advances*, 2015, **5**, 83239-83285.
88. L. Zhu, C. Tian, D. Yang, X. Jiang and R. Yang, *Electroanalysis*, 2008, **20**, 2518-2525.
89. J. C. Ndamanisha and L. P. Guo, *Analytical Chimica Acta*, 2012, **747**, 19-28.
90. S. Zhou, H. Shi, X. Feng, K. Xue and W. Song, *Biosensors Bioelectronics*, 2013, **42**, 163-169.
91. A. Nsabimana, J. Lai, S. Li, P. Hui, Z. Liu and G. Xu, *Analyst*, 2017, **142**, 478-484.
92. M. M. Abdel-Galeil, H. S. El-Desoky, E. M. Ghoneim and A. Matsuda, *Journal of The Electrochemical Society*, 2017, **164**, H1003-H1012.
93. S. Zhou, H. Xu, J. Liu, Y. Wei, X. Ma, Z. Han and H. Chen, *Chemical Physics*, 2021, **542**, 111074.
94. Y. Zhang, G. I. N. Waterhouse, Z. P. Xiang, J. Che, C. Chen and W. Sun, *Food Chem*, 2020, **326**, 126976.
95. M. Dai, B. Haselwood, B. D. Vogt and J. T. La Belle, *Analytical Chimica Acta*, 2013, **788**, 32-38.
96. Q. Zhang, C. Zhang, Y. Ying and J. Ping, *Food Control*, 2021, **129**, 108203.
97. Y. Lyu, S. Gan, Y. Bao, L. Zhong, J. Xu, W. Wang, Z. Liu, Y. Ma, G. Yang and L. Niu, *Membranes*, 2020, **10**, 128.
98. Z. Jiang, X. Xi, S. Qiu, D. Wu, W. Tang, X. Guo, Y. Su and R. Liu, *Journal of Materials Science*, 2019, **54**, 13674-13684.
99. H. Wang, B. Yuan, T. Yin and W. Qin, *Analytica Chimica Acta*, 2020, **1129**, 136-142.
100. S. Han, D. Wu, S. Li, F. Zhang and X. Feng, *Advanced Materials*, 2014, **26**, 849-864.
101. A. Guirguis, J. W. Maina, X. Zhang, L. C. Henderson, L. Kong, H. Shon and L. F. Dumée, *Materials Horizons*, 2020, **7**, 1218-1245.
102. S. H. Kazemi, E. Ghodsi, S. Abdollahi and S. Nadri, *Materials Science and Engineering: C*, 2016, **69**, 447-452.
103. Y. Zhang, Q. Wan and N. Yang, *Small*, 2019, **15**, e1903780.
104. N. Baig, A. Waheed, M. Sajid, I. Khan, A.-N. Kawde and M. Sohail, *Trends in Environmental Analytical Chemistry*, 2021, **30**, e00120.
105. Y. Li, L. Shi, G. Han, Y. Xiao and W. Zhou, *Sensors and Actuators B: Chemical*, 2017, **238**, 945-953.
106. Y. Zhu, K. Kang, Y. Jia, W. Guo and J. Wang, *Microchimica Acta*, 2020, **187**, 669.
107. S. Salagare, P. S. Adarakatti, Y. Venkataramanappa and A. S. A. Almalki, *Ionics*, 2021, DOI: 10.1007/s11581-021-04355-9.
108. Y. Liu, X. Zhao, C. Wang, L. Zhang, M. Li, Y. Pan, Y. Fu, J. Liu and H. Lu, *Journal of Materials Chemistry A*, 2018, **6**, 18267-18275.
109. H. Wang, X. Bo and L. Guo, *Sensors and Actuators B: Chemical*, 2014, **192**, 181-187.
110. J. H. Yoon, H. J. Park, S. H. Park, K. G. Lee and B. G. Choi, *Carbon Letters*, 2019, **30**, 73-80.
111. Q. He, S. R. Das, N. T. Garland, D. Jing, J. A. Hondred, A. A. Cargill, S. Ding, C. Karunakaran and J. C. Claussen, *ACS Applied Materials & Interfaces*, 2017, **9**, 12719-12727.
112. J. Lin, Z. Peng, Y. Liu, F. Ruiz-Zepeda, R. Ye, E. L. Samuel, M. J. Yacaman, B. I. Yakobson and J. M. Tour, *Nature Communications*, 2014, **5**, 5714.
113. N. T. Garland, E. S. McLamore, N. D. Cavallaro, D. Mendivelso-Perez, E. A. Smith, D. Jing and J. C. Claussen, *Applied Materials & Interfaces*, 2018, **10**, 39124-39133.
114. Z. Wan, N.-T. Nguyen, Y. Gao and Q. Li, *Sustainable Materials and Technologies*, 2020, **25**, e00205.
115. C. Zhang, J. Ping and Y. Ying, *Science of the total environment*, 2020, **714**, 136687.
116. S. Sharma, S. K. Ganeshan, P. K. Pattnaik, S. Kanungo and K. N. Chappanda, *Materials Letters*, 2020, **262**, 127150.
117. Z. Wan, M. Umer, M. Lobino, D. Thiel, N.-T. Nguyen, A. Trinchi, M. J. A. Shiddiky, Y. Gao and Q. Li, *Carbon*, 2020, **163**, 385-394.
118. Y. Yang, Y. Song, X. Bo, J. Min, O. S. Pak, L. Zhu, M. Wang, J. Tu, A. Kogan, H. Zhang, T. K. Hsiai, Z. Li and W. Gao, *Nature Biotechnology*, 2020, **38**, 217-224.
119. R. M. Torrente-Rodriguez, H. Lukas, J. Tu, J. Min, Y. Yang, C. Xu, H. B. Rossiter and W. Gao, *Matter*, 2020, **3**, 1981-1998.
120. S. L. James, *Chemical Society Reviews*, 2003, **32**, 276-288.
121. F. Zhao, T. Sun, F. Geng, P. Chen and Y. Gao, *International Journal of Electrochemical Science*, 2019, **14**, 5287-5304.
122. L. L. Gao, W. J. Sun, X. M. Yin, R. Bu and E. Q. Gao, *Microchimica Acta*, 2019, **186**, 762.
123. J. Wang, S. Liu, J. Luo, S. Hou, H. Song, Y. Niu and C. Zhang, *Frontiers in Chemistry*, 2020, **8**, 594093.
124. C.-S. Liu, J. Li and H. Pang, *Coordination Chemistry Reviews*, 2020, **410**, 213222.
125. C. H. Chuang and C. W. Kung, *Electroanalysis*, 2020, **32**, 1885-1895.
126. B. Cagnon, M. S. Secula and Ş. S. Bayazit, in *Carbon-based material for environmental protection and remediation*, eds. M. Bartoli, M. Frediani and L. Rosi, IntechOpen, 2020, DOI: 10.5772/intechopen.91355.
127. D. Liu, W. Gu, L. Zhou, L. Wang, J. Zhang, Y. Liu and J. Lei, *Chemical Engineering Journal*, 2022, **427**, 131503.
128. J. M. Gonçalves, P. R. Martins, D. P. Rocha, T. A. Matias, M. S. S. Julião, R. A. A. Munoz and L. Angnes, *Journal of Materials Chemistry C*, 2021, **9**, 8718-8745.
129. L. Cui, J. Wu and H. Ju, *ACS Applied Materials & Interfaces*, 2014, **6**, 16210-16216.
130. J. Xu, J. Xia, F. Zhang and Z. Wang, *Electrochimica Acta*, 2017, **251**, 71-80.
131. Y. Baikeli, X. Mamat, M. Wumaer, M. Muhetaer, H. A. Aisa and G. Hu, *Journal of The Electrochemical Society*, 2020, **167**, 116513.
132. Y. Liu, J. Fan, F. He, X. Li, T. Tang, H. Cheng, L. Li and G. Hu, *Surfaces and Interfaces*, 2021, **27**.

133. J. Xu, M. Lv, J. Yang, Q. Chuai, X. Cao, J. Xia, F. Zhang, T. Zou and Z. Wang, *Sensors and Actuators B: Chemical*, 2021, **349**.
134. S. Zheng, D. Wu, L. Huang, M. Zhang, X. Ma, Z. Zhang and S. Xiang, *Journal of Applied Electrochemistry*, 2019, **49**, 563-574.
135. M. Zhang, M. Li, W. Wu, J. Chen, X. Ma, Z. Zhang and S. Xiang, *New Journal of Chemistry*, 2019, **43**, 3913-3920.
136. Y. Wang, M. Qiao, X. Mamat, X. Hu and G. Hu, *Materials Research Bulletin*, 2021, **136**, 111131.
137. L. Liu, L. Liu, Y. Wang and B. C. Ye, *Talanta*, 2019, **199**, 478-484.
138. L. Xiao, R. Xu, Q. Yuan and F. Wang, *Talanta*, 2017, **167**, 39-43.
139. J. Zhang, J. Liu, Y. Zhang, F. Yu, F. Wang, Z. Peng and Y. Li, *Microchimica Acta*, 2017, **185**, 78.